Carbohydrate Polymers 103 (2014) 228–233

Contents lists available at ScienceDirect

Carbohydrate Polymers

journal homepage: www.elsevier.com/locate/carbpol

Effects of amylose and phosphate monoester on aggregation structures of heat-moisture treated potato starches

Binjia Zhang [a], Yue Zhao [a], Xiaoxi Li [a,*], Panfeng Zhang [a], Lin Li [a], Fengwei Xie [b], Ling Chen [a,*]

[a] Ministry of Education Engineering Research Center of Starch & Protein Processing, Guangdong Province Key Laboratory for Green Processing of Natural Products and Product Safety, College of Light Industry and Food Sciences, South China University of Technology, Guangzhou 510640, China
[b] Australian Institute for Bioengineering and Nanotechnology, The University of Queensland, Brisbane, QLD 4072, Australia

ARTICLE INFO

Article history:
Received 14 July 2013
Received in revised form
15 December 2013
Accepted 16 December 2013
Available online 25 December 2013

Keywords:
Potato starch
Heat-moisture treatment
Aggregation structure
Amylose
Phosphate monoester

ABSTRACT

For three cultivars of potato starch, heat-moisture treatment (HMT) displayed an influence on the aggregation structures at different scale levels. With HMT, the granular morphology of potato starch granules remained similarly, and an increase in the average repeat distance of semi-crystalline lamellae was observed. The crystalline structure and birefringence were also affected. Moreover, the polymorphic transformation (B → A + B) could be related to dehydration, whereas the decrease in the degree of crystallinity might be resulted from the rupture of hydrogen bonds. Interestingly, amylose could act as the backbone of the aggregation structures of potato starch to provide resistance to HMT, but phosphate monoester could promote the destruction during HMT. In addition, compared with amylose, phosphate monoester played a more significant role in changing the average repeat distance of semi-crystalline lamellae (long period) during HMT.

1. Introduction

Starch is a natural polymer and is widely used in many industrial fields, either as a main raw material or as an additive. In general, starch consists of two major polymer components, namely amylose and amylopectin. Amylose is a relatively long linear D-glucan containing 99% α-1,4 linkages and 1% α-1,6 linkages, whereas amylopectin is a highly branching D-glucan containing 95% α-1,4 linkages and 5.0% α-1,6 linkages (Damager, Engelsen, Blennow, Møller, & Motawia, 2010; Pérez & Bertoft, 2010). These two polymers form the amorphous and crystalline regions in the starch granule (Zhang, Zhao, et al., 2014). Due to the diversities in starch source, composition, structure, and properties, starches are suitable for various applications contributing to different functionalities (Hoover, 2010). However, the application of native starch is limited because of the undesirable defects caused by the structural characteristics, such as poor solubility, low heat and shear resistance, uncontrolled paste consistency, high tendency toward retrogradation and gelling, and low freeze–thaw stability of pastes (BeMiller, 1997; Lawal, 2009). To overcome these shortcomings, various techniques of starch modification, including chemical, physical and enzymatic methods, are widely used to improve the inherent characteristics of starch (BeMiller, 1997; Pu et al., 2011; Zhang, Chen, Zhao, & Li, 2013).

Heat-moisture treatment (HMT) is defined as a physical modification method that involves the treatment of starch granules at a low moisture level (<35%) and at a temperature (84–120 °C) above the glass transition temperature (T_g) but below the gelatinization temperature for a certain period of time (15 min–16 h) (Gunaratne & Hoover, 2002). HMT has gained great attention as one of the physical modification techniques to modify the physicochemical properties of starch without destroying its granular structure. According to a previous report (Hoover, 2010), HMT had an influence on the crystalline structure, starch chain interactions, granular swelling, amylose leaching, viscosity, gelatinization parameters, retrogradation, and susceptibility toward acid and α-amylase hydrolysis of cereal, tuber, and legume starches. Furthermore, there are many factors that can affect the extents of changes in the structure and properties of starch during HMT, such as the starch composition, organization of amylose and amylopectin within the native granule, and conditions (e.g. temperature, moisture, and time). It is worth noting that the semi-crystalline lamellae of starch can be disrupted by HMT (Vermeylen, Goderis, & Delcour, 2006). Additionally, HMT can lead to a reduction in the gelatinization endotherm and total crystallinity of potato starch (Hoover &

* Corresponding authors. Tel.: +86 20 8711 3252; fax: +86 20 8711 3252.
E-mail addresses: xxlee@scut.edu.cn (X. Li), felchen@scut.edu.cn, zbw9383@163.com (L. Chen).

0144-8617/$ – see front matter © 2013 Elsevier Ltd. All rights reserved.
http://dx.doi.org/10.1016/j.carbpol.2013.12.055

Vasanthan, 1994; Miyoshi, 2002; Stute, 1992), and a shift from B- to A-type crystalline structure (Vermeylen et al., 2006). Therefore, the aggregation structural characteristics of starch can be affected by HMT. The aggregation structures (mainly lamellar structure and crystalline structure) of starch play a key role in determining the properties (Kim & Huber, 2010; Zhang, Li, Liu, Xie, & Chen, 2013b). Particularly, the crystalline structure can affect the enzymatic resistivity of starch (resistant starch content) (Zhang, Chen, et al., 2013) which displays a nutritional relevance and potential health benefits.

Potato starch is one of the worldwide starch resources and has been widely used in foods and non-food industries. For further improving the properties of native potato starch by using HMT and thus extending the industrial applications of potato starch, it is indispensable to investigate the influences of starch granular components (amylose, and phosphate monoester, etc.) on the aggregation structures of HMT treated potato starch. However, there have been few studies on the detailed comparison of the changes in aggregation structures of HMT treated potato starch as affected by the amylose and phosphate monoester contents. Normally, potato starch contains more phosphate monoester than cereal starches (Blennow & Engelsen, 2010; Wickramasinghe, Blennow, & Noda, 2009) and the crystallites of potato starch are more susceptible to disruption by HMT (Hoover, 2010). This indicates that phosphate monoester may be a determinant on the extent of influence by HMT on the structures of potato starch. Nonetheless, the role of amylose during HMT, especially the concurrent effect of amylose and phosphate monoester on the aggregation structures of potato starch, has not been clarified so far. This is undesirable for further investigations of the relationship between the aggregation structures and the properties of potato starch to extend the application of potato starch in foods and other starch-based products. Therefore this work involves the selection of three cultivars of potato starch which had different amylose and phosphorus contents for HMT, in order to investigate the HMT-induced changes in the granular morphology, lamellar structure, and crystalline structure of these starches as affected by the amylose and phosphorus contents.

2. Materials and methods

2.1. Materials

Three cultivars of potato starch (Qing 168, Qing 5, and Feiwuruita) from Qinghai Province, China were used in this experiment, and were referred to as Potato-1, Potato-2, and Potato-3 respectively. They were supplied by Sanjiang Group Co., Ltd. (Xining, China). A moisture analyzer (MA35, Sartorius Stedim Biotech GmbH, Germany) was used to determine the moisture content (MC) of each sample.

2.2. Amylose content

The apparent amylose contents of native and HMT treated potato starches were determined using the AACC method 61-03 (10) through the spectrophotometric detection, which is based on blue color formation upon the reaction of amylose with iodine. A UV-3802 spectrophotometer (UNICO, New Jersey, USA) was used to measure the color at 620 nm. All the measurements were done in triplicates.

2.3. Phosphorus content

The phosphorus contents of potato starches were obtained with an energy dispersive X-ray spectrometer (EDX) of EVO18 scanning electron microscope (ZEISS, Oberkochen, Germany) operated at a voltage of 10.0 kV.

2.4. Heat-moisture treatment

Each potato starch was premixed with distilled water to reach certain moisture content (MC, ~30%) and treated in a reactor (Model No. 4545, Parr Instrument Company, Moline, Illinois, USA) at 110 °C with stirring for 30 min. After that, all the samples were air dried at 45 °C for 48 h and ground for further analysis. The HMT treated potato starches were referred to as Potato-1-HMT, Potato-2-HMT, and Potato-3-HMT, respectively.

2.5. Aggregation structures of native and heat-moisture treated potato starches

2.5.1. Scanning electron microscopy (SEM)

Granular morphology was observed using an EVO18 scanning electron microscope (ZEISS, Oberkochen, Germany) operated at a voltage of 10.0 kV. All the samples were coated with a thin gold layer before the microscopic examination.

2.5.2. Small-angle X-ray scattering (SAXS)

SAXS experiments were performance according to the method in our previous reports (Zhu, Li, Chen, & Li, 2012; Zhang, Xiong, et al., 2014) with proper modification. An SAXSess system (Anton-Paar GmbH, Austria) equipped with a PW3830 X-ray generator (PANalytical B.V., The Netherlands), operated at 50 mA and 40 kV, using Cu Kα radiation with a wavelength of 0.1542 nm as the X-ray source was used. The starch slurries with a MC of about 60% were prepared and equilibrated at 20 °C for 24 h before the analysis. Each sample was placed into a paste sample cell and measured for 10 min. The data, recorded using an image plate, were collected by the IP Reader software program with a PerkinElmer® Storage Phosphor System. All data were normalized, and the background intensity and smeared intensity were removed using the SAXSquant 3.0 software program for further analysis.

2.5.3. Polarized light microscopy (PLM)

A polarized light microscope (Axioskop 40 Pol/40A Pol, ZEISS, Oberkochen, Germany) equipped with a 35 mm SLA camera (Power Shot G5, Canon, Tokyo, Japan) was used to obtain the polarized light microscopic images. Each sample was dispersed as 10 mg of starch in 1 mL of distilled water in a glass vial and observed at 500× magnification (50 × 10). A drop of starch suspension was transferred onto a slide, covered by a cover slip.

2.5.4. X-ray diffraction (XRD)

XRD analysis was performed with a Xpert PRO diffractometer (PANalytical B.V., The Netherlands), operated at 40 mA and 40 kV, using Cu Kα radiation with a wavelength of 0.1542 nm as the X-ray source. The scanning of diffraction angle (2θ) was from 5° to 40° with a scanning speed of 10°/min and a scanning step of 0.033°. The samples were equilibrated in an oven (DHG-9145A, Shanhai Bluepard Instruments Co., Ltd., China) at 40 °C for 24 h and the MC of all the samples was about 15% before the analysis. The relative crystallinity (RC) of each sample was calculated using the method by Hermans and Weidinger (1948).

3. Results and discussion

3.1. Amylose and phosphorus contents

Table 1 shows the amylose and phosphorus contents of the different native potato starches. The amylose content is one of the main factors that affect the physicochemical properties of

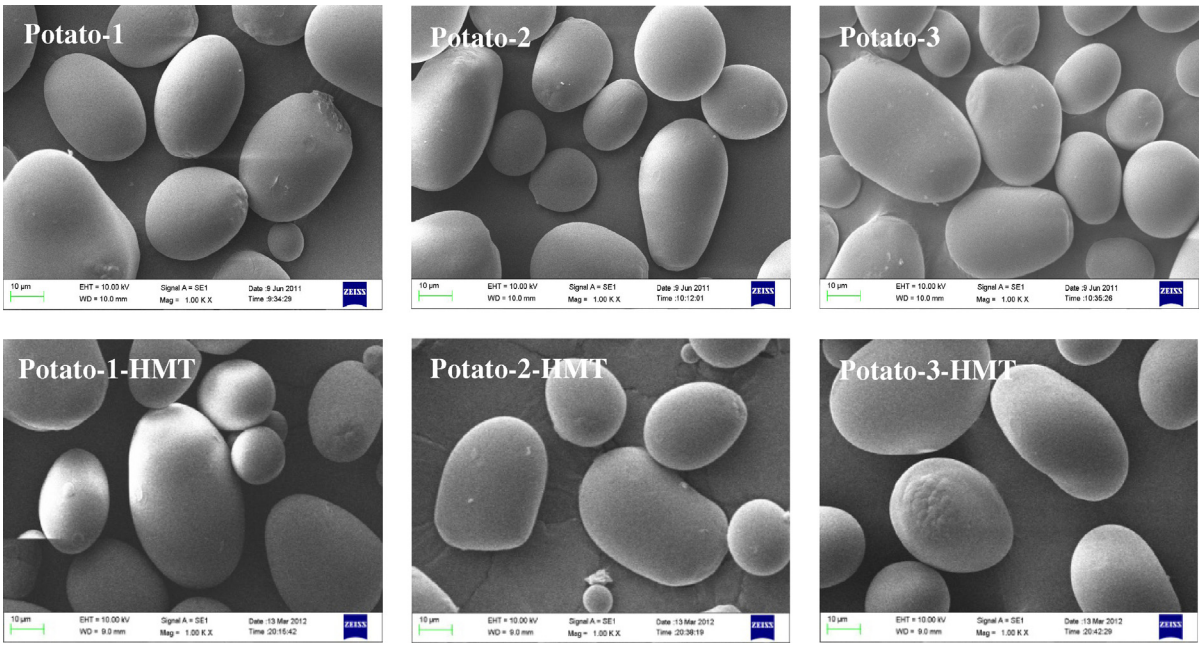

Fig. 1. SEM images of native potato starches and HMT treated potato starches at 1000× magnification.

Table 1
Amylose and phosphorus contents of the potato starches.

Samples	Potato-1	Potato-2	Potato-3
Amylose content (%)	34.8	32.3	26.8
Phosphorus content (%)	0.28	0.17	0.37

starch, and a higher amylose content may lead to a higher gelatinization temperature, lower peak and breakdown viscosities (Pycia, Juszczak, & Galkowska, 2012), and a higher content of resistant starch. As seen from Table 1, the amylose content of Potato-1 was 34.8%, which was the highest among these samples, whilst Potato-2 contained more amylose than Potato-3. Commonly, potato starch has more phosphate monoester than cereal starches (Blennow & Engelsen, 2010; Wickramasinghe et al., 2009). In the present study, the phosphorus content followed the order Potato-3 > Potato-1 > Potato-2. The phosphorus monoester content had the same trend as the phosphorus content, since phosphorus existed in the form of phosphorus monoester in potato starch.

3.2. Aggregation structural characteristics of native and heat-moisture potato starches

The aggregation structure (supramolecular structure) of starch mainly contains the lamellar structure, and the crystalline structure (Zhang, Li, et al., 2013). It is found that the structure of native starch is organized in four length scales: the molecules (~0.1 nm), the lamellar structure (8–9 nm), the growth rings (~0.1 μm), and the whole granular morphology (μm) (Pikus, 2005). Depending on the packing of the amylopectin side chains into double helices or the amylose single helices, the crystalline structure of starch is classified as A-, B-, C-, or V-type, which has been shown by X-ray diffraction (XRD). The C-type crystalline structure is actually a combination of the A- and B-type structures, while the V-type crystalline structure describes the amylose single helices co-crystallized with compounds such as iodine, dimethyl sulfoxide (DMSO), alcohols, or fatty acids (Buleon, Colonna, Planchot, & Ball, 1998; Gernat, Tadosta, & Damaschun, 1990; Kim & Huber, 2010; Luengwilai & Beckles, 2009; Nara & Komiya, 1983; Sarko & Wu, 1978).

3.2.1. Granular morphology

The SEM images of the native and HMT treated potato starches are shown in Fig. 1. It is seen that the native starch granules were mostly in ellipsoidal shape along with some to be more rounded, and the HMT treated potato starches displayed similar granular morphology as their native counterparts.

3.2.2. Lamellar structural characteristics

The semi-crystalline lamellae (alternating crystalline and amorphous lamellae) in the hydrated starch granule are widely detected by the SAXS technique (Blazek & Gilbert, 2011; Lopez-Rubio, Htoon, & Gilbert, 2007; Suzuki, Chiha, & Yano, 1997; Zhu et al., 2012), related to the difference in electron density between the crystalline lamellae and the amorphous lamellae. The value of q of the peak at round 0.6 nm^{-1}, which is related to the difference in electron density between the crystalline lamellae and the amorphous lamellae, can be used to calculate the average repeat distance (d) of the semi-crystalline lamellae (long period) according to the Woolf-Bragg's equation ($d = 2\pi/q$) (Suzuki et al., 1997; Zhu et al., 2012). The SAXS patterns and the related parameters of native and HTM treated potato starches are shown in Fig. 2 and Table 2. It is seen that the peaks for the native potato starches were located between the q values of 0.6888 nm^{-1} and 0.6995 nm^{-1}, corresponding to Bragg distances (d) between 8.978 nm and 9.117 nm. Furthermore, the HMT treated potato starches possessed larger values of d than the native counterparts. The increase in d can be further expressed in percentage as $\Delta d\,(\%) = (d_{HMT} - d_{Native})/d_{Native}$, (where d_{Native} and d_{HMT} is the average repeat thicknesses of the semi-crystalline lamellae in the native and HMT treated potato starches respectively).

As shown in Table 2, Δd showed the same trend as the increase of phosphate monoester content. It is widely accepted that, compared with cereal starches, tuber starches, such as potato starch, normally have a higher content of phosphate monoester, which is mainly located on C_3 and C_6 of the glucose residues (Blennow & Engelsen, 2010; Kozlov, Blennow, Krivandin, & Yuryev, 2007; Wickramasinghe et al., 2009). The stability of the crystalline structure of the starch granule can be influenced by the phosphate groups, and particularly, phosphate groups at the C-3 position of the glucose units seems to play a significant role by inducing strain

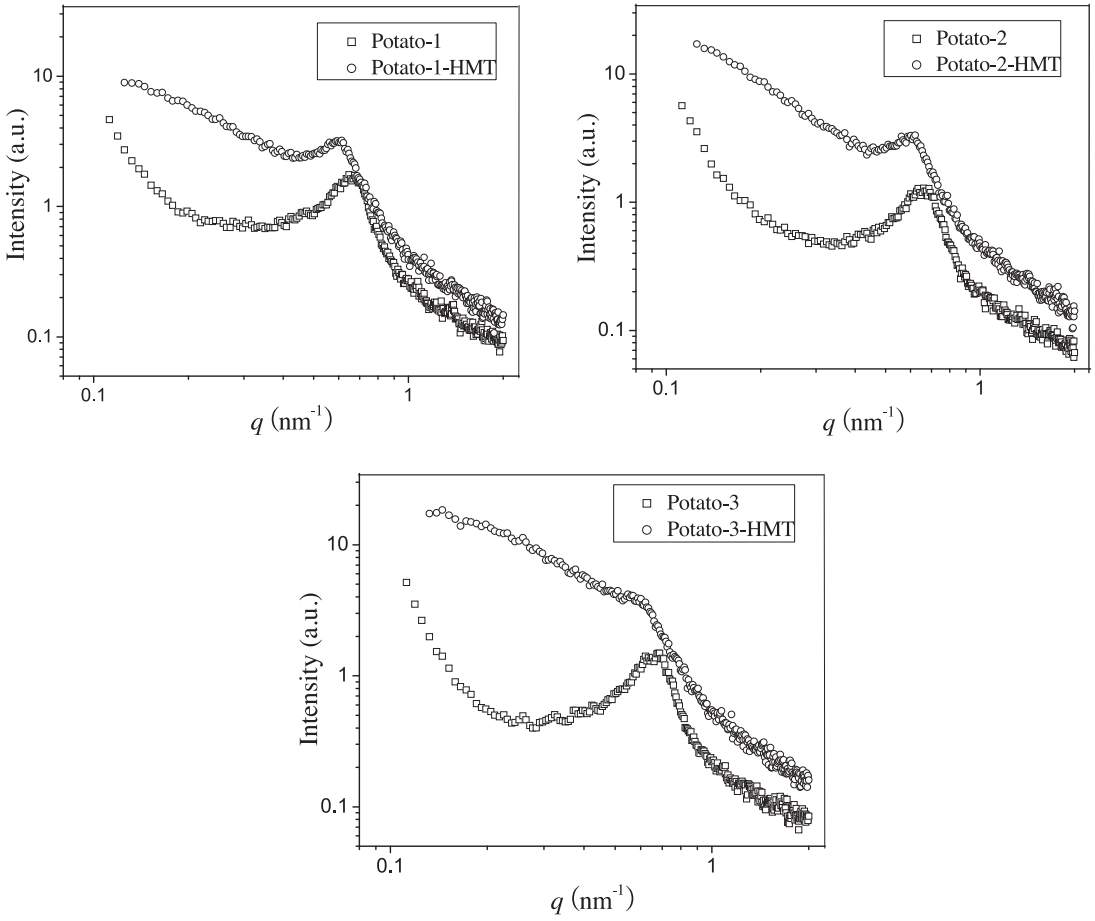

Fig. 2. Double-logarithmic SAXS patterns of native and HTM treated potato starches.

Table 2
Lorentz corrected SAXS parameters and relative crystallinity (*RC*) of the native and HMT treated potato starches.

Samples	Potato-1	Potato-1-HMT	Potato-2	Potato-2-HMT	Potato-3	Potato-3-HMT
q_{peak} (nm^{-1})	0.6888	0.6290	0.6995	0.6535	0.6956	0.6207
d (nm)	9.117	9.984	8.978	9.610	9.028	10.118
Δd (%)		9.51		7.04		12.07
RC (%)	29.1	16.8	35.4	20.4	37.0	20.0
ΔRC (%)		42.3		42.4		45.9

in crystalline starch and resulting in helix unfolding (Blennow & Engelsen, 2010), which have a close relationship with the crystalline lamellae.

It is also noted from the results of Tables 1 and 2 that Δd decreased non-linearly with the decrease of amylose content. Based on previous studies (Jane, Xu, Radosavljevi, & Seib, 1992; Kozlov et al., 2007), amylose is randomly interspersed as in single molecules rather than in bundles among amylopectin molecules, and can co-crystallize with the amylopectin. Thus amylose molecules can provide a resistance to HMT because the amylose molecules act as the backbones of the aggregation structures of starch. According to the final changes in Δd of the three potato starches, during HMT, the phosphate monoester should play a more significant role in the change in the lamellar repeat thickness compared with the amylose, and a higher content of phosphate monoester could lead to a higher degree of change in the average repeat thickness of the semi-crystalline lamellae.

Normally, the high degree of ordering in the flawless semi-crystalline lamellae can lead to the appearance of a SAXS scattering peak with fine visibility at around 0.6 nm^{-1}. As seen from Fig. 2, HMT caused a reduction in the visibility of the peak at around 0.6 nm^{-1}, indicating that, compared with the native counterparts, the HMT treated potato starches contained more flawed semi-crystalline lamellae and a lower degree of ordering. Additionally, Potato-3-HMT presented the least visible peak in its SAXS pattern. This might be attributed to both the smallest amount of amylose and the largest amount of phosphate monoester existing in Potato-3, as amylose molecules could act as the backbones of the aggregation structures to provide a resistance to HMT and phosphate monoester could promote the destruction of HMT.

3.2.3. *Crystalline structure*

Maltese crosses (birefringence) can be observed when native starch granules are exposed under polarized light. This is attributed to the anisotropy in the starch granule because of the orderly arranged starch molecules of crystalline regions and the disorderly arranged starch molecules of amorphous regions. Moreover, the intensity of birefringence depends on the granular size, relative crystallinity, and microcrystalline orientation (Zhang, Li, et al., 2013). Fig. 3 shows the polarized light microscopic pictures of the native and HTM treated potato starch samples. It is seen that all the HMT treated potato starches displayed lower intensity of

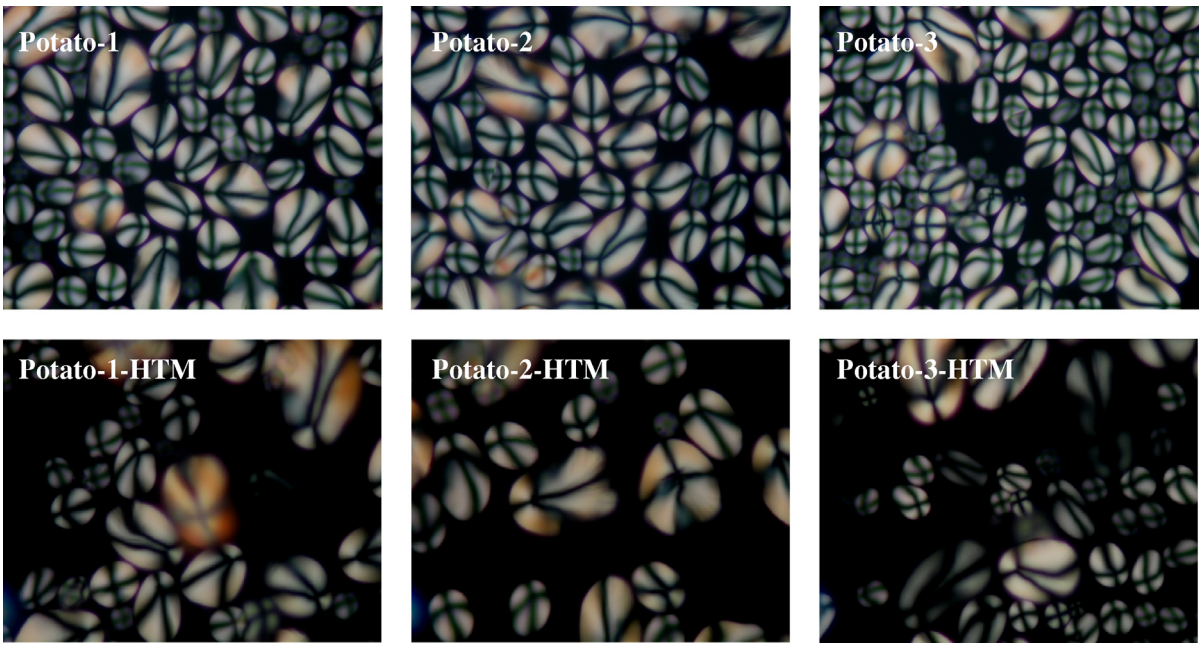

Fig. 3. Polarized light microscopic pictures of native and HTM treated potato starches (500×).

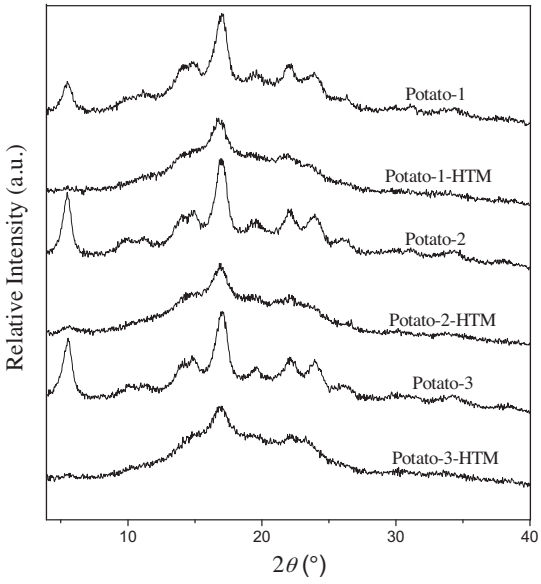

Fig. 4. XRD patterns of native and HTM treated potato starches.

birefringence than the native counterparts, indicating the destruction by HMT to the crystalline structure of potato starch. After HMT, some of the starch granules became larger and the centers of Maltese crosses were less obvious.

Starch molecules form crystalline and amorphous regions in the starch granule. The XRD patterns of amorphous parts of starch are dispersive, while those of crystalline parts of starch always have sharp peaks (Gernat et al., 1990). For a specific type of starch, a certain XRD pattern can be obtained; in other words, each type of crystalline structure of starch displays its own XRD pattern. Fig. 4 shows the XRD patterns of the native and HMT treated potato starches. As presented in Fig. 4, all the native potato starches displayed a typical B-type crystalline structure with main diffraction peaks at around 5.6, 17, 22 and 24° (2θ), while all the HMT treated potato starches had the main diffraction peaks at around 17 and 22–24° (2θ), indicating a A + B crystalline structure (Parada & Aguilera, 2012; Vermeylen et al., 2006). The change in the X-ray pattern could be related to dehydration. That is, the vaporization of the 36 water molecules in the central channel of the B-unit cell resulted in the movement of a pair of double helices toward the central channel, leading to the polymorphic transformation from B to A + B (Gunaratne & Hoover, 2002; Vermeylen et al., 2006). Moreover, a decrease in the diffraction peak was observed for the HMT treated potato starch samples, which could be related to the rupture of the hydrogen bonds, causing the adjacent double helices to move apart and resulting in orientations that were not in a perfect parallel crystalline array (Hoover & Vasanthan, 1994).

Furthermore, the change in *RC* during HMT is also shown in Table 2. Compared with the native potato starches, the HMT treated samples showed a drastic decrease in RC. To be more accurate, the RC of native potato starches was in the range from 29.1% to 37.0%, while that of HMT treated potato starches ranged from 16.8 to 20.4%. The percentage of decrease in *RC*, i.e. ΔRC (%, $=(RC_{Native} - RC_{HMT})/RC_{Native}$, where RC_{Native} and RC_{HMT} are the RC values of the native and HMT treated starches respectively), was further used to understand the changes by HMT to the different potato starches. It is seen that HMT caused the similar degree of destruction to the crystalline structures of Potato-1 and Potato-2, whereas the crystalline structure of Potato-3 underwent the most severe destruction during HMT.

As discussed above, amylose can co-crystallize with amylopectin (Jane et al., 1992; Kozlov et al., 2007), providing a resistance to HMT, while phosphate monoester promoted the effect of HMT on the crystalline structure of potato starch, due to the strain in crystalline starch and the helix unfolding induced by the phosphate groups at the C-3 position of the glucose units (Blennow & Engelsen, 2010). As a result, with a larger amount of phosphate monoester, a higher degree of destruction to the aggregation structures of starch, including the crystalline structure, could be resulted from HMT. Combined with the results of Tables 1 and 2, it can be concluded that during HMT the similar degree of decrease in the *RC* values for Potato-2 and Potato-1 should be due to the concurrent influences of amylose and phosphate monoester, and the highest degree of reduction in the *RC* value for Potato-3 during HMT was also expected since Potato-3 contained the highest amount of phosphate monoester but the least amount of amylose. Therefore, the difference in amylose and phosphate monoester contents caused

different degrees of destruction by HMT to the crystalline structure of potato starches, and the decrease in *RC* resulted from the concurrent effects of amylose and phosphate monoester.

4. Conclusion

This study involves the use of three cultivars of potato starch, which varied in the amylose content and the phosphate monoester content. For these potato starches, HMT displayed an influence on the aggregation structures at different scale levels. The HMT treated potato starch granules displayed similar the granular morphology as the native counterparts, and the HMT treated potato starches possessed a larger average repeat distance (*d*) of semi-crystalline lamellae than the native counterparts. Moreover, HMT led to destructions to the crystalline structure of potato starch, and the centers of Maltese crosses of starch granules became less apparent. While all the native potato starches displayed a typical B-type crystalline structure, all the HMT treated potato starches showed an A + B crystalline structure and a lower *RC* value. This might be related to the vaporization of the water molecules in the central channel of the B-unit and the rupture of the hydrogen bonds respectively.

Furthermore, while HMT caused a similar degree of destruction to the crystalline structure of Potato-1 and Potato-2, the highest degree of destruction to these structural characteristics was seen for Potato-3. This could be related to the differences in the phosphate monoester content (Potato-3 > Potato-1 > Potato-2) and the amylose content (Potato-1 > Potato-2 > Potato-3), and the concurrent effect of amylose and phosphate monoester on the crystalline structure of potato starch. One explanation for this could be that amylose molecules might act as the backbones of the aggregation structures of potato starch to provide a resistance to HMT but the phosphate groups, particularly the phosphate groups at the C-3 position of the glucose units, could influence the stability of the crystalline structure of the starch granule by inducing strain in crystalline starch and resulting in helix unfolding. Moreover, during HMT, the phosphate monoester played a more significant role in the change of the lamellar repeat thickness compared with the amylose, and more phosphate monoester led to a higher degree of change in the average repeat thickness of the semi-crystalline lamellae.

These results provide new information on the aggregation structural changes of different potato starches by HMT and the concurrent roles of amylose and phosphate monoester in these changes. As these changes could be related to the changes in properties, the information here is expected to facilitate better application of various potato starches in the fields such as foods and starch-based materials.

Acknowledgements

The authors would like to acknowledge the National Natural Science Funds of China (Nos. 31130042, 31071503, 31271824), the National Science and Technology Supporting Program Projects (2012BAD33B04), the Special R&D Funds for the Doctoral Discipline Stations in Universities, Ministry of Education (20120172110014), the Ministry of Education Program for Supporting New Century Excellent Talents (NCET-12-0193), the Office of Education of Guangdong Province Science and Technology Innovation (Key) Projects in Universities (2012CXZD0006) and the Fundamental Research Funds for the Central Universities (2013ZG0009).

References

BeMiller, J. N. (1997). Starch modification: Challenges and prospects. *Starch/Stärke*, *49*(4), 127–131.

Blazek, J., & Gilbert, E. P. (2011). Application of small-angle X-ray and neutron scattering techniques to the characterisation of starch structure: A review. *Carbohydrate Polymers*, *85*, 281–293.

Blennow, A., & Engelsen, S. B. (2010). Helix-breaking news: Fighting crystalline starch energy deposits in the cell. *Trends in Plant Science*, *15*(4), 236–240.

Buleon, A., Colonna, P., Planchot, V., & Ball, S. (1998). Starch granules: Structure and biosynthesis. *International Journal of Biological Macromolecules*, *23*, 85–112.

Damager, I., Engelsen, S. B., Blennow, A., Møller, B. L., & Motawia, M. S. (2010). First principles insight into the α-glucan structures of starch: Their synthesis, conformation and hydration. *Chemical Reviews*, *110*, 2049–2080.

Gernat, C., Tadosta, S., & Damaschun, G. (1990). Supramolecular structure of legume starches revealed by X-ray scattering. *Starch/Stärke*, *42*(5), 175–178.

Gunaratne, A., & Hoover, R. (2002). Effect of heat-moisture treatment on the structure and physicochemical properties of tuber and root starches. *Carbohydrate Polymers*, *49*, 425–437.

Hermans, P. H., & Weidinger, A. (1948). Quantitative X-ray investigations on the crystallinity of cellulose fibers. A background analysis. *Journal of Applied Physics*, *19*, 491–506.

Hoover, R. (2010). The impact of heat-moisture treatment on molecular structures and properties of starches isolated from different botanical sources. *Critical Reviews in Food Science and Nutrition*, *50*, 835–847.

Hoover, R., & Vasanthan, T. (1994). Effect of heat-moisture treatment on the structure and physicochemical properties of cereal, legume and tuber starches. *Carbohydrate Research*, *252*, 33–53.

Jane, J., Xu, A., Radosavljevi, M., & Seib, R. A. (1992). Location of amylose in normal starch granules. I. Susceptibility of amylose and amylopectin to cross-linking reagents. *Cereal Chemistry*, *69*, 405–410.

Kim, K. S., & Huber, K. C. (2010). Physicochemical properties and amylopectin fine structures of A- and B-type granules of waxy and normal soft wheat starch. *Journal of Cereal Science*, *51*, 256–264.

Kozlov, S. S., Blennow, A., Krivandin, A. V., & Yuryev, V. P. (2007). Structural and thermodynamic properties of starches extracted from GBSS- and GWD suppressed potato lines. *International Journal of Biological Macromolecules*, *40*, 449–460.

Lawal, O. S. (2009). Starch hydroxyalkylation: Physicochemical properties and enzymatic digestibility of native and hydroxypropylated finger millet (*Eleusine coracana*) starch. *Food Hydrocolloids*, *23*, 415–425.

Lopez-Rubio, A., Htoon, A., & Gilbert, E. P. (2007). Influence of extrusion and digestion on the nanostructure of high-amylose maize starch. *Biomacromolecules*, *8*, 1564–1572.

Luengwilai, K., & Beckles, D. M. (2009). Structural investigations and morphology of tomato fruit starch. *Journal of Agricultural and Food Chemistry*, *57*, 282–291.

Miyoshi, E. (2002). Effect of heat-moisture treatment and lipids on gelatinization and retrogradation of maize and potato starches. *Cereal Chemistry*, *79*, 72–77.

Nara, S., & Komiya, T. (1983). Studies on the relationship between water-saturated state and crystallinity by the diffraction method for moistened potato starch. *Starch/Stärke*, *35*, 407–410.

Parada, J., & Aguilera, J. M. (2012). Effect of native crystalline structure of isolated potato starch on gelatinization behavior and consequently on glycemic response. *Food Research International*, *45*, 238–243.

Pérez, S., & Bertoft, E. (2010). The molecular structures of starch components and their contribution to the architecture of starch granules: A comprehensive review. *Starch/Stärke*, *62*, 389–420.

Pikus, S. (2005). Small angle X-ray scattering (SAXS) study's the structure of starch and starch products. *Bio-polymers and Conducting Polymers*, *13*(5), 82–86.

Pu, H. Y., Chen, L., Li, X. X., Xie, F. W., Yu, L., & Li, L. (2011). An oral colon-targeting controlled release system based on resistant starch acetate: Synthetization, characterization, and preparation of film-coating pellets. *Journal of Agricultural and Food Chemistry*, *59*, 5738–5745.

Pycia, K., Juszczak, L., & Galkowska, D. (2012). Physicochemical properties of starches obtained from polish potato cultivars. *Starch/Stärke*, *64*(2), 105–114.

Sarko, A., & Wu, H. C. (1978). The crystal structures of A-, B-, and C-polymorphs of amylose and starch. *Starch/Stärke*, *30*, 73–78.

Stute, R. (1992). Hydrothermal modification of starches: The difference between annealing and heat-moisture treatment. *Starch/Stärke*, *44*, 205–214.

Suzuki, T., Chiha, A., & Yano, T. (1997). Interpretation of small angle X-ray scattering from starch on the basis of fractals. *Carbohydrate Polymers*, *34*, 357–363.

Vermeylen, R., Goderis, B., & Delcour, J. A. (2006). An X-ray study of hydrothermally treated potato starch. *Carbohydrate Polymers*, *64*, 364–375.

Wickramasinghe, H. A. M., Blennow, A., & Noda, T. (2009). Physico-chemical and degradative properties of in-planta re-structured potato starch. *Carbohydrate Polymers*, *77*, 118–124.

Zhang, B. J., Chen, L., Zhao, Y., & Li, X. X. (2013). Structure and enzymatic resistivity of debranched high temperature-pressure treated high-amylose corn starch. *Journal of Cereal Science*, *57*, 348–355.

Zhang, B. J., Li, X. X., Liu, J., Xie, F. W., & Chen, L. (2013). Supramolecular structure of A- and B-type granules of wheat starch. *Food Hydrocolloids*, *31*, 68–73.

Zhang, B. J., Xiong, S. X., Li, X. X., Li, L., Xie, F. W., & Chen, L. (2014). Effect of oxygen glow plasma on supramolecular and molecular structures of starch and related mechanism. *Food Hydrocolloids*, *37*, 69–76.

Zhang, B. J., Zhao, Y., Li, X. X., Li, L., Xie, F. W., & Chen, L. (2014). Supramolecular structural changes of waxy and high-amylose cornstarches heated in abundant water. *Food Hydrocolloids*, *35*, 700–709.

Zhu, J., Li, L., Chen, L., & Li, X. X. (2012). Study on supramolecular structural changes of ultrasonic treated potato starch granules. *Food Hydrocolloids*, *29*, 116–122.